

# **Heat Release Effects on Shear-Layer Growth and Entrainment**

**J. C. Hermanson, M. G. Mungal, P. E. Dimotakis**

# Heat Release Effects on Shear-Layer Growth and Entrainment

J. C. Hermanson,\* M. G. Mungal,† and P. E. Dimotakis‡  
*California Institute of Technology, Pasadena, California*

The effects of heat release were studied in a planar, gaseous reacting mixing layer formed between two subsonic freestreams; one containing hydrogen in an inert diluent, the other containing fluorine in an inert diluent. Sufficiently high concentrations of hydrogen and fluorine reactants were employed to produce adiabatic flame temperature rises of up to 940 K (adiabatic flame temperature of 1240 K absolute). Although the displacement thickness of the layer for a zero streamwise pressure gradient showed an increase with increasing heat release, the actual thickness of the mixing layer at a given downstream location was not observed to increase and, in fact, was characterized by a slight thinning. The overall entrainment into the layer was seen to be substantially reduced by heat release. The large-scale vortical nature of the flow appeared to persist over all levels of heat release in this investigation. Imposition of a favorable pressure gradient, though resulting in additional thinning of the layer, was observed to have no resolvable effect on the amount of chemical product formation and hence on the mixing.

## I. Introduction

THIS investigation was concerned with heat-release effects in a subsonic, gas-phase, turbulent, plane, reacting shear layer at high Reynolds number. The work was an extension of earlier work in the same facility.<sup>1-3</sup> The flow consisted of a two-dimensional mixing layer with gas-phase freestreams; one stream carrying a given concentration of hydrogen in an inert diluent, the other carrying fluorine in an inert diluent. The reaction  $H_2 + F_2 \rightarrow 2HF$  is highly exothermic so that reactant concentrations of 1%  $H_2$  and 1%  $F_2$ , each in an  $N_2$  diluent, produce an adiabatic flame temperature rise of 93 K above ambient. Results will be presented here corresponding to fluorine concentrations of up to 6% and hydrogen concentrations of up to 24%, with a maximum adiabatic flame temperature rise of 940 K (corresponding to an adiabatic flame temperature of 1240 K absolute).

In earlier, low heat release work by Mungal et al.<sup>1-3</sup> with flame temperature rises of up to 165 K, no coupling of heat release with the fluid mechanics could be observed, as manifested by the layer growth rate, entrainment, and discernible large-scale structure dynamics. In those works, the chemical reaction could be considered as a diagnostic used to infer the amount of molecular mixing without disturbing the overall properties of the layer. In the work reported here, the heat release was much larger and the effects of the heat release itself on the properties of the shear layer were investigated. The highest heat-release cases reported here produced a time-averaged temperature change sufficient to reduce the mean density in the center of the layer by a factor of nearly 3, assuming constant pressure conditions.

## II. Experimental Facility and Instrumentation

The experimental apparatus is described in detail by Mungal and Dimotakis<sup>2</sup> and also by Hermanson.<sup>4</sup> It is a blowdown facility in which premixed volumes of fluorine in an inert diluent and hydrogen in an inert diluent are discharged through sonic orifices to maintain a constant mass flux. Each stream enters a settling and contraction section for turbulence suppression with the high-speed stream emerging from a 6:1 contraction with an exit area of  $5 \times 20$  cm, and the low-speed stream emerging from a 4:1 contraction with a  $7.5 \times 20$ -cm exit area. The two streams meet at the tip of a splitter plate, with a trailing edge included angle of 3.78 deg. The high-speed freestream turbulence level was measured<sup>2</sup> to be about 0.6% rms.

To offset the freestream density difference, which results from large amounts of hydrogen in one stream, the densities of the freestreams were matched, for most cases, by using as diluent a mixture of nitrogen and a small amount of helium on the fluorine side, and a mixture of nitrogen with a small amount of argon on the hydrogen side. This also served to match the heat capacities of the two freestreams to an accuracy of approximately 6-10%, as the freestream absolute reactant concentrations were estimated to be accurate to 3-5% by Mungal and Dimotakis.<sup>2</sup>

Runs were performed with a nominal high-speed flow velocity of 22 m/s and a freestream speed ratio of  $U_2/U_1 \approx 0.4$ . In practice, the high-speed flow velocity varied from run to run up to about 5% from the nominal high-speed velocity; the corresponding variation in the low-speed stream velocity was typically less than 6%. The freestream speed ratio for each run was typically within 4% of the nominal value. These variations were a result of differences in gas constants of the various mixtures, although the sonic metering orifices were adjusted for each run to minimize these variations. The measuring station was positioned at  $x = 45.7$  cm downstream of the splitter-plate trailing edge. The Reynolds number at the measuring station was typically  $Re_{\delta_1} \approx 6 \times 10^4$ , based on the freestream velocity difference, the 1% thickness of the mean temperature profile, and the cold freestream kinematic viscosity. The 1% thickness,  $\delta_1$ , of the temperature or concentration field<sup>2,5</sup> is defined here as the transverse width of the layer at which the time-averaged temperature rise is 1% of the maximum time-averaged temperature rise and was used in this investigation as the

Presented as Paper 85-0142 at the AIAA 23rd Aerospace Sciences Meeting, Reno, NV, Jan. 14-17, 1985; received Sept. 18, 1985; revision received Sept. 15, 1986. Copyright © 1985 by J. C. Hermanson. Published by the American Institute of Aeronautics and Astronautics, Inc., with permission.

\*Graduate Student, Aeronautics; currently Engineer, Applied Physics Laboratory, University of Washington. Member AIAA.

†Research Fellow, Aeronautics; currently, Assistant Professor, Mechanical Engineering Department, Stanford University. Member AIAA.

‡Professor, Aeronautics and Applied Physics. Member AIAA.

principal measure of layer width. The quality  $\delta_1$  has been shown<sup>2</sup> to correlate well with the visual thickness  $\delta_{vis}$  (Ref. 6) of the layer. The value of the Reynolds number based on  $\delta_1$  is well above that for the mixing transition as reported by Bernal et al.,<sup>7</sup> Breidenthal,<sup>8</sup> and Konrad.<sup>9</sup> The corresponding Reynolds number based on the high-speed freestream velocity and on the downstream distance was  $Re_x \approx 6 \times 10^5$ . A diagram of the shear-layer geometry is shown in Fig. 1.

Temperature data were recorded with a rake of eight 2.5- $\mu\text{m}$ -diam platinum-10% rhodium cold wires, with a typical wire span of 1.5 mm, welded to Inconel prongs. For some runs, a rake of 25- $\mu\text{m}$ -diam Chromel-Alumel thermocouples was employed. It was found that the 2.5  $\mu\text{m}$  resistance wires in the hottest regions did not survive in runs in which the adiabatic flame temperature rise exceeded approximately 600 K. Both the cold wire and thermocouple probe rakes were positioned across the transverse extent of the layer. The probes were equally spaced at nominal intervals of 1 cm, which sufficed to capture the mean temperature rise profile. The total data rate for the resistance wires was 80 kHz, corresponding to 10 kHz per probe. The thermocouples were sampled at 500 Hz each, for a total data rate of 4 kHz; their considerably lower frequency response not warranting a higher rate.

Thermocouples produce a voltage proportional to the junction temperature and normally do not require calibration. The resistance wires were calibrated as described previously<sup>1,2</sup> using a hot and cold jet of known temperature. The two measurements provided calibration constants to convert voltage to temperature rise. An additional correction was applied to the output signal voltage in the present experiments to account for the nonlinearity in the resistivity of the platinum-10% rhodium wire element at elevated temperatures.<sup>10</sup> It was determined that for neither the thermocouples nor the resistance wires was there significant radiation error for the temperatures in this investigation.<sup>11</sup> Both probes, however, were influenced by heat conduction to the support prongs, which could have resulted in excursions from the mean temperature being in error by as much as 10-20% for the cold wires and up to 40% for the thermocouples. Both diagnostics, however, produced accurate mean temperatures, as during a small fraction of the course of the run (before data acquisition began) the tips of the support prongs equilibrated to the local mean value. Good agreement (typically within 5%) was obtained in runs in which both sets of probes were employed. Errors resulting from differences in the thermal conductivities between the freestreams were established to be small.<sup>4</sup>

In addition to the temperature probes, a schlieren system was utilized for concurrent flow visualization. The beam width utilized was sufficient to illuminate a 25-cm length of the shear layer. A circular source mask and a circular hole spatial filter were used in place of the conventional source slit and knife edge in an effort to give equal weights to gradients in index of refraction in all directions and to better resolve the large-scale structure of the flow. The hole sizes were increased with increasing flow temperature to optimize (reduce) sensitivity as needed. High time-resolution spark schlieren photographs were taken with a spark source ( $\sim 3\text{-}\mu\text{s}$  duration), synchronized with a motor-driven 35-mm camera, at a rate of approximately three frames per second.

The mean velocity profile was measured for most runs by a pitot probe rake of 15 probes connected to a miniature manometer bank filled with fluorine-resistant oil (Hooker Chemical Fluorolube FS-5) with a time response of 2-3 s, adequate to yield a reliable mean dynamic pressure profile during each 6-s run. The bank was photographed by a second motor-driven 35-mm camera. The photographic data were digitized and reduced to mean velocity profiles. This technique of measuring the pitot pressure was estimated to be accurate to 5%. Rebollo<sup>12</sup> estimated that the accuracy of extracting mean velocities from pitot pressures in noncon-

stant density flows is about 4-5%. This estimate was made for a shear flow with a freestream density ratio of  $\rho_2/\rho_1 = 7$ . In the present experiment, the density ratio of the cold freestreams to the hot layer center was at most 3, suggesting that the Rebollo error estimate represents an upper bound under these conditions.

Finally, the streamwise static pressure gradient was monitored by measuring the pressure difference between two downstream locations on the low-speed sidewall with a Datametrics type 573 fluorine-resistant Barocel sensor. The high-speed sidewall was kept horizontal for all runs and the low-speed sidewall was adjusted for the desired streamwise pressure gradient. The wedge-like geometry of the planar shear-layer displacement allows this simple means of accommodating or imposing any desired pressure gradient. Most of the runs in the present investigation were performed with the low-speed sidewall adjusted to the requisite divergence angle to ensure a zero streamwise pressure gradient. For some runs at high heat release, the walls were left fixed at the angle required for zero pressure gradient at zero heat release, producing a favorable streamwise pressure gradient (accelerating flow) as a result of the combustion displacement effects due to volume expansion.

### III. Chemistry

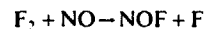
The chemical reaction utilized in the present investigation is effectively



This yields a temperature rise of 93 K for 1%  $\text{F}_2$  and 1%  $\text{H}_2$  in  $\text{N}_2$  diluent under constant pressure, adiabatic conditions (this is the so-called adiabatic flame temperature rise). The chemical reaction is actually comprised of two second-order chain reactions:



Proper chain initiation requires some free F atoms, which were generated in these experiments by premixing a trace amount of nitric oxide into the hydrogen-carrying stream. This allows the reaction



which provides the required small F atom concentration in the layer to sustain proper ignition and combustion. For all runs in this investigation, the NO concentration was maintained at 3% of the freestream fluorine concentration.

For all flows reported here, the resulting chemical time scales were fast compared with the fluid mechanical time scales. The chemical time scales for the reaction, over the entire range of concentrations, were determined using the CHEMKIN chemical kinetics program.<sup>13</sup> The chemical rate

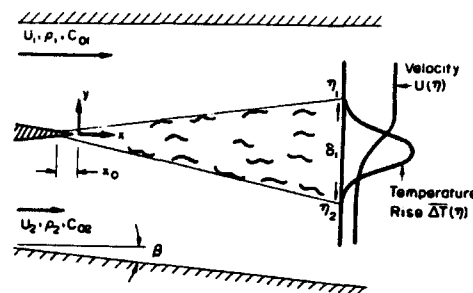


Fig. 1 Turbulent shear-layer geometry.

data for the reactions involved were taken from Refs. 14 and 15. The Damköhler number (ratio of mixing time to chemical time) based on the local, large-scale characteristic time ( $\delta_1/\Delta U$ , where  $\Delta U$  is the freestream velocity difference) ranged from 25 to 130 with increasing reactant concentrations. The Damköhler number based on the time of flight from the location of the mixing transition to the measuring station [ $(x-x_r)/U_c$ , where  $U_c$  is the mean convection speed,  $(U_1+U_2)/2$ ] varied from 95 to 470. Taking the transition Reynolds number to be  $Re_{\delta_1} = 2 \times 10^4$  gives  $x_r = 14.2$  cm. The recent work of Mungal and Frierle<sup>16</sup> suggests that the chemistry can be regarded as being fast when the Damköhler numbers exceed 10 and 40 for the large scales and time of flight, respectively. Chemical kinetics are, consequently, not an issue in the present investigation, where the chemistry is much faster as a result of the higher reactant concentrations and combustion temperatures.

The stoichiometric mixture ratio  $\phi$  is defined here as the volume of high-speed fluid required to react completely with a unit volume of low-speed fluid. This is the same as the ratio of the low-speed freestream molar concentration  $c_{02}$  to the high-speed freestream molar concentration  $c_{01}$  divided by the low- to high-speed stoichiometric ratio, i.e.

$$\phi = \frac{c_{02}/c_{01}}{(c_{02}/c_{01})_s} = c_{02}/c_{01}$$

In this case the molar stoichiometric ratio for the hydrogen-fluorine reaction is unity.

#### IV. Results and Discussion

##### A. Growth Rate and Entrainment

The low-speed sidewall divergence required for zero streamwise pressure gradient is a direct measure of the displacement thickness of the layer  $\delta^*$ , where  $\delta^*/(x-x_0)$  indicates the tangent of the angle  $\beta$  by which the low-speed freestream line is shifted owing to the presence of the shear layer (see Fig. 1). Note that the displacement thickness is less than zero for a layer with no heat release, and increases steadily with heat release, as shown in Fig. 2. The parameter  $(\rho_0 - \bar{\rho})/\rho_0$  represents the mean normalized density reduction in the layer due to heat release, where  $\bar{\rho}$  is the mean density in the layer and  $\rho_0 = (\rho_1 + \rho_2)/2$  is the average (cold) density of the freestreams. The mean density is defined as

$$\bar{\rho} = \rho_0 \int_{y_2}^{y_1} \frac{T_0}{(T_0 + \Delta T)} dy$$

where  $y_{1,2}$  are the 1% points of the mean temperature profile on the high- and low-speed sides, respectively;  $T_0$  the ambient temperature; and  $\Delta T$  the time-averaged temperature rise at each point across the layer. This calculation neglects the small changes in pressure across the layer by taking the pressure to be constant. Alternatively, the effects of heat release could be quantified by use of the parameter  $\tau \equiv \langle \Delta T \rangle / T_0$ , which represents, at constant pressure, the additional volume created by heat addition.  $\langle \Delta T \rangle$  denotes the mean temperature rise in the layer, which is defined here in a similar fashion to the mean density.

The observed 1% temperature profile thickness at zero pressure gradient is plotted vs the mean density in the layer in Fig. 3. It may be worth noting that the actual shear-layer thickness, in spite of large heat release and large density changes, does *not* increase with heat release and, in fact, shows a slight decrease, even though the displacement thickness (Fig. 2) increases with heat release. This effect was noted by Wallace<sup>17</sup> and was observed in the present set of experiments in which the maximum mean flow temperature increase was about three times greater than in Ref. 17. Since it was difficult to hold the speed ratio at exactly 0.40 from run to run and also because the density ratio of the

freestreams was slightly different from unity for some runs, each data point in Fig. 3 has been corrected by normalization with the expected growth rate for a cold layer with the identical speed and density ratio, using the formula derived in Ref. 18.

$$\frac{\delta}{x} = \epsilon \left( \frac{1-r}{1+s^{1/2}r} \right) \left( 1+s^{1/2} - \frac{1-s^{1/2}}{1+2.9[(1+r)/(1-r)]} \right)$$

where  $s = \rho_2/\rho_1$ ,  $r = U_2/U_1$ , and  $\epsilon$  is a constant. A linear least-squares fit to the data in Fig. 3 suggests that the layer thinning, for a mean density reduction of 40% may be as high as 15%. The largest mean density reduction presented in this work,  $(\rho_0 - \bar{\rho})/\rho_0 = 0.38$ , corresponds to a run with an adiabatic flame temperature rise of  $\Delta T_f = 940$  K and a mean temperature rise in the layer of  $\langle \Delta T \rangle = 248$  K. No dependence of the thinning trend on stoichiometric mixture ratio was observed.

The slight reduction in layer thickness with increasing heat release is also confirmed by the mean velocity data. Sample velocity profiles, at different heat release but identical speed and density ratios, are presented in Fig. 4. It can be seen that the hotter layer is noticeably steeper in maximum slope, in agreement with Ref. 17. Normalization of this maximum slope by the freestream velocity difference gives the vorticity thickness  $\delta_\omega$  of the layer,

$$\frac{1}{\delta_\omega} = \frac{1}{\Delta U} \left( \frac{dU}{dy} \right)_{\max}$$

A plot of the vorticity thickness variation with heat release, again corrected for variations in speed ratio and density

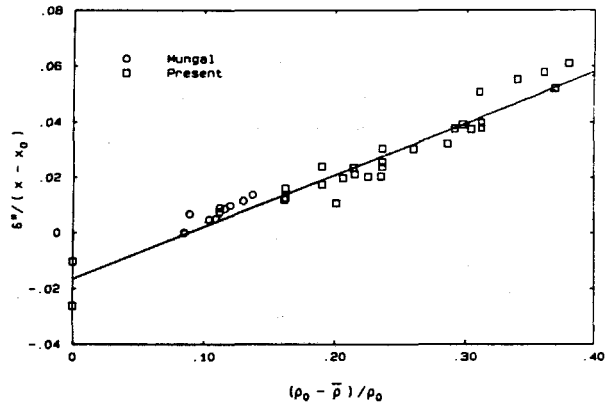


Fig. 2 Layer displacement vs heat release.

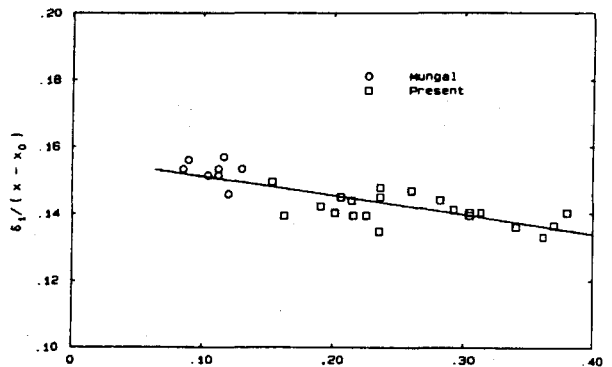


Fig. 3 Temperature profile thickness growth rate vs heat release:  $\circ - \Delta T_f = 0$ ,  $(\rho_0 - \bar{\rho})/\rho_0 = 0$ ;  $\square - \Delta T_f = 457$  K,  $(\rho_0 - \bar{\rho})/\rho_0 = 0.286$ .

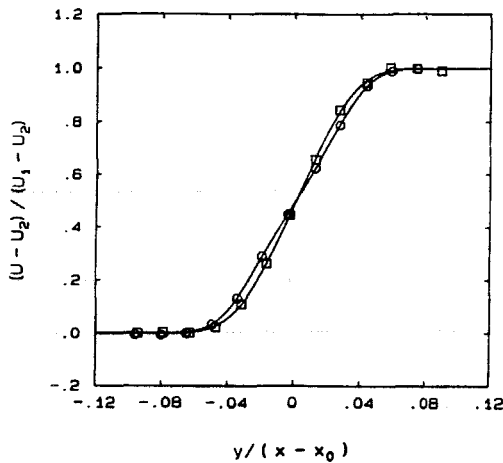


Fig. 4 Mean velocity profile comparison, nonreacting and at high heat release.

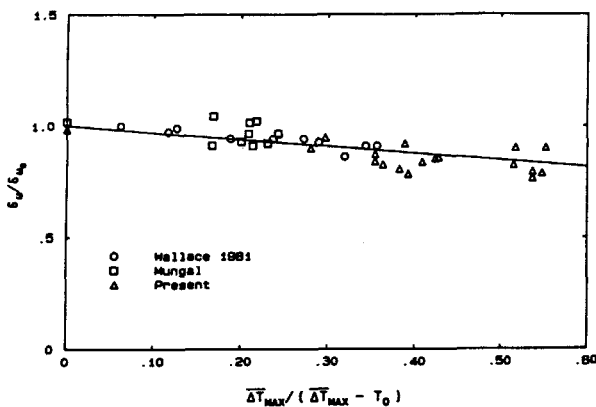


Fig. 5 Normalized vorticity thickness comparison with Ref. 17.

ratio, is shown in Fig. 5. Each point is normalized by a representative value for the vorticity thickness at zero heat release. The portion of the present results at moderate heat release, including some unpublished data of Mungal, are seen to be in good agreement with Ref. 17. Since the data of Ref. 17 were originally given in terms of  $\Delta T_{max}/T_0$ , the maximum time-averaged temperature rise over the ambient temperature, it was necessary to use the quantity  $\Delta T_{max}/(\Delta T_{max} + T_0)$  for the abscissa parameter of Fig. 5. This quantity is slightly different than  $(\rho_0 - \bar{\rho})/\rho_0$  because the density is not a linear function of the temperature rise, but nonetheless yields a comparable thinning effect to Fig. 3.

Direct numerical simulations of a reacting mixing layer performed by McMurtry et al.<sup>19</sup> also suggest a decrease in layer thickness when exothermic reactions occur, in qualitative agreement with the present results. Those simulations indicate both a decrease in the width of the calculated product concentration profile as well as a steepening in the mean velocity profile with increasing heat release.

Experiments performed at higher temperatures than those in this work by Pitz and Daily<sup>20</sup> in a combustng mixing layer formed downstream of a rearward-facing step indicated that the vorticity thickness did not appear to change between their cold runs and high heat-release runs. However, Keller and Daily<sup>21</sup> report that, in a reacting mixing layer between a cold premixed reactant stream and a preheated combustion product stream, the vorticity thickness increases significantly with increasing temperature. The reasons for the discrepancy between those results and the ones reported here are not

clear at this writing. However, two important differences exist between the experimental conditions of those investigations and the present work. First, Pitz and Daily<sup>20</sup> and Keller and Daily<sup>21</sup> studied shear layers formed between unequal density fluids, unlike the present study with matched freestream densities. Second, those experiments, in contrast to the present investigation, were performed in a constant area duct in which a pressure gradient was allowed to develop.

A complicating factor in any discussion of growth rate is the location of the virtual origin  $x_0$ , since the relevant similarity downstream coordinate is in fact  $y/(x-x_0)$ . The trends in layer thinning reported here do allow the possibility that some of the effects could be accounted for by a shift in the virtual origin with heat release. The location of the virtual origin  $x_0$  was determined visually from the intersection of the apparent layer edges as revealed by spark schlieren photographs (see Sec. IV. B). These results did not, however, suggest any systematic change in the location of the virtual origin with heat release, and a representative value of  $x_0 = -3.2$  cm was used for all normalizations in this investigation.<sup>4</sup> Initial conditions can have a significant effect on layer growth as has been shown, for example, by Browand and Latigo;<sup>22</sup> see also Batt,<sup>23</sup> Bradshaw,<sup>24</sup> and the discussion in the review paper by Ho and Huerre.<sup>25</sup>

One implication of the fact that the layer width does not increase with increasing temperature is that, since the density in the layer is substantially reduced but the layer does not grow faster, the total volumetric entrainment of freestream fluid into the layer must also be reduced greatly by heat release. The amount of entrainment into the layer can be calculated from the mean velocity and density (i.e., temperature) profiles as follows:

$$\frac{\dot{V}}{U_1(x-x_0)} = \int_{\eta_2}^{\eta_1} \frac{\rho U}{\rho_0 U_1} d\eta$$

where  $\dot{V}$  is the volume flux into the layer per unit span,  $x-x_0$  the downstream coordinate, and  $\eta = y/(x-x_0)$  the shear-layer similarity coordinate. This expression assumes that the layer is self-similar at the station at which the integral is performed. The quantity  $\rho U$  was computed as  $\bar{\rho} \bar{U}$ , which was used here as an approximation for the density-velocity correlation  $\rho U$ .

Results from Mungal et al.<sup>3</sup> suggest that there is a Reynolds number dependence on product formation. Since the growth rate does appear to be a function of the product formation (i.e., heat release), strictly speaking, the flow would not be expected to be exactly self-similar. An alternate method,<sup>18,26</sup> which approximates the overall entrainment, is to use the geometry of the layer as shown in Fig. 1 to derive

$$\frac{\dot{V}}{U_1(x-x_0)} = \eta_1 - r(\eta_2 + \tan\beta)$$

where  $r = U_2/U_1$ ,  $\eta_{1,2}$  are the similarity coordinate edges of the shear layer, and  $\beta$  is the deflection angle of the low-speed sidewall. A common difficulty of both methods is that of selecting values for  $\eta_1$  and  $\eta_2$ . One reasonable choice is the pair of points corresponding to the 1% edges of the temperature profile. Resulting calculations for choices of 1 and 10% points in the temperature profiles, for both the integral and geometric methods, are plotted in Fig. 6. It can be seen that, regardless of the choice of edge reference points, the inference is that the entrainment into the layer is strongly reduced as a function of heat release, amounting to about 50% for a mean density in the layer of 40% below its nominal cold value. The decrease in entrainment with heat release is greater than that suggested by considering only the increase in volume and taking the entrainment to be proportional to  $1/(\tau+1)$ . That the entrainment reduction is in ex-

cess of the mean density reduction suggests that the decrease in entrainment flux more than compensates for the additional displacement due to density change.

**B. Large-Scale Structure Dynamics**

Figure 7 shows time traces of temperature rise from the rake of cold wires. Both runs are at  $\phi = 1$ . The data in Fig. 7a are from a run with 2% F<sub>2</sub> and 2% H<sub>2</sub> with an adiabatic flame temperature rise of  $\Delta T_f = 186$ K. Figure 7b shows the results of a run with 6% F<sub>2</sub> and 6% H<sub>2</sub> with an adiabatic flame temperature rise of  $\Delta T_f = 553$ K. The quantity  $\Delta T_{max}$  is the highest recorded temperature rise of the data represented in each figure. At this amount of heat release, the flow dynamics still appeared to be dominated by large-scale structures separated by cold tongues of fluid that extend well into the layer. These findings are consistent with the earlier results at low temperatures.<sup>1-3</sup> Spark schlieren photographs of the first 25 cm of the layer are presented in Fig. 8,

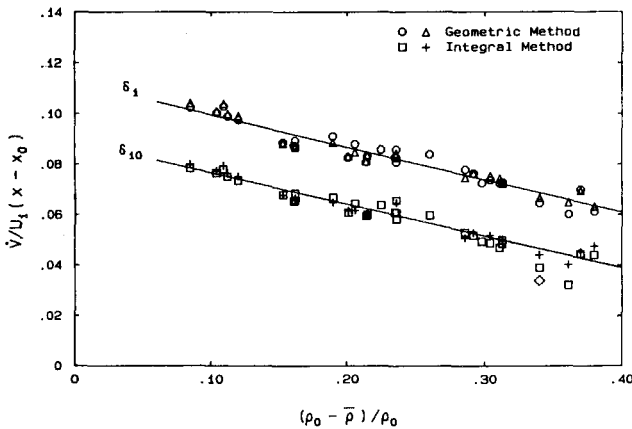


Fig. 6 Dependence of volumetric entrainment on heat release.

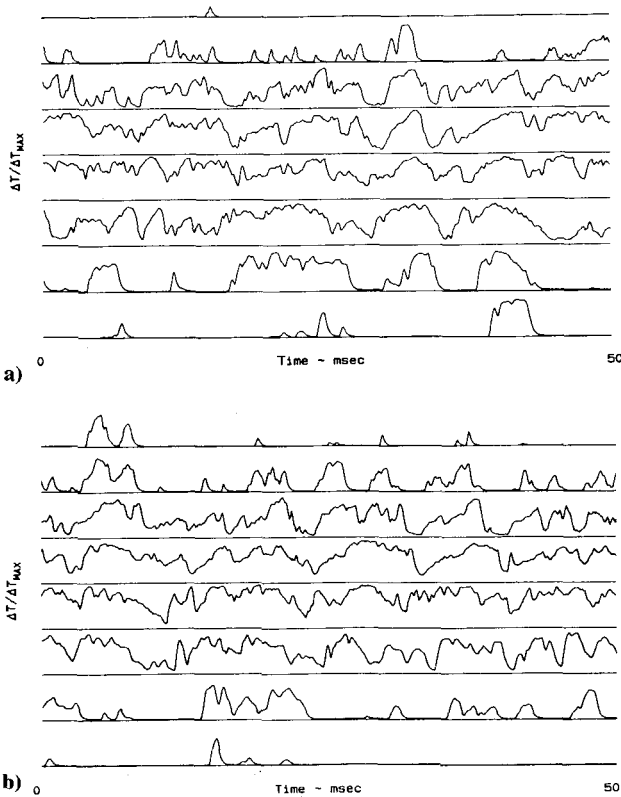


Fig. 7 Temperature vs time traces. a) 2% F<sub>2</sub>:2% H<sub>2</sub>,  $\Delta T_f = 186$ K,  $\Delta T_{max} = 171$  K; b) 6% F<sub>2</sub>: 6% H<sub>2</sub>,  $\Delta T_f = 553$  K,  $\Delta T_{max} = 496$  K.

representing conditions of both low and high heat release. Figure 8a corresponds to the same conditions as Fig. 7a. In Fig. 8b is shown a 6% F<sub>2</sub> and 24% H<sub>2</sub> run with an adiabatic flame temperature rise of 847 K, a higher temperature than in Fig. 7b. The large-scale structure is evident in both photographs. Furthermore, that the structures appear well defined in the schlieren photographs suggests that they retain their predominantly two-dimensional nature. Ganji and Sawyer<sup>27</sup> and Pitz and Daily<sup>20</sup> continued to observe the large-scale structures behind a rearward-facing step at higher temperatures, corresponding to adiabatic flame temperatures of up to about 1650 K absolute. Keller and Daily<sup>21</sup> also observed that well-ordered structures were present for all values of heat release in their investigations.

**V. Pressure Gradient Results**

It has been argued that, in reacting flows with substantial density variations and appreciable pressure gradients, an additional mixing mechanism might be operative, resulting from a possible relative acceleration between light fluid elements and heavy fluid elements.<sup>28,29</sup> The efficacy of such a mechanism would of course depend on the scales at which the density variations would be observed and their relation to the viscous small scales of the flow. If the hot/cold fluid elements are very closely spaced, viscous effects might not permit large relative motions to be established and little or no augmentation of the mixing will be observed. These issues were addressed, in part, in the experiments discussed below.

Setting the sidewalls for zero pressure gradient for the cold flow yields a naturally induced favorable pressure gradient in the case of flow with heat release. In this investigation, such favorable pressure gradient runs were made at reactant concentrations of up to 6% H<sub>2</sub> and 6% F<sub>2</sub>, corresponding to a flame temperature rise of 553 K. This was sufficient to induce a pressure increment  $\Delta p$  over the distance from the splitter-plate tip to the measuring station of about one-half of  $\frac{1}{2}\rho_0 U_2^2$ , the low-speed freestream dynamic head. This caused the high-speed velocity to increase from 21.2 to 22.3 m/s and the low-speed velocity to increase from 8.2 to 10.3 m/s between the splitter tip and the measuring station.

The resulting mean temperature profiles are presented in Fig. 9 with and without pressure gradient. The layer is thinned by the pressure gradient, as would be expected in accelerating flow. It can be seen, however, at least for the values of heat release and pressure gradient reported here, that the favorable pressure gradient appears to yield no

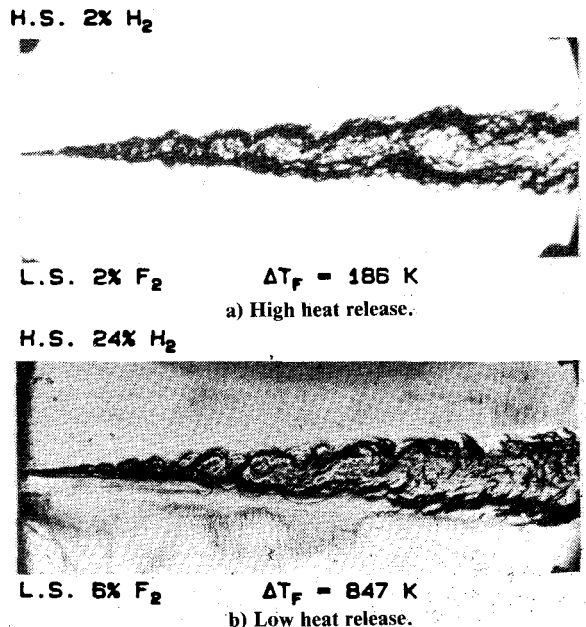


Fig. 8 Spark schlieren photographs at low and high heat release.

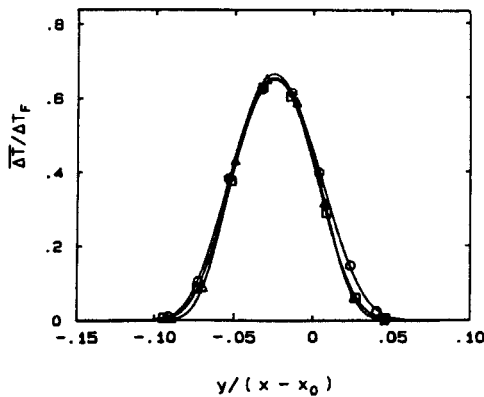


Fig. 9 Pressure gradient effect on mean temperature profile, 6%  $F_2$ :6% $H_2$ . ○— $dp/dx=0$ ; □— $\Delta dp/dx < 0$ .

significant change in either the maximum time-averaged temperature or in the total amount of product formed, which is related to the area under the mean temperature profile normalized by the layer thickness.<sup>2,4</sup> Temperature profiles at lower temperatures also show no systematic changes in the total amount of product resulting from pressure gradient, at least to within the estimated reproducibility and accuracy of the data (3–5%).

## VI. Conclusions

The results of this investigation suggest that the growth rate of a chemically reacting shear layer with heat release does not increase and, in fact, decreases slightly with increasing heat release. In the presence of an increase in the shear-layer displacement thickness as a result of heat release, one might expect a commensurate increase in shear layer thickness. The implication is that the decrease in the entrainment flux due to volume expansion must more than compensate for the displacement effect.

The imposition of a favorable pressure gradient is found to not have any noticeable effect on the amount of mixing and chemical production in the layer.

## Acknowledgments

The assistance of C. E. Frieler as well as the expert help of Mr. Earl E. Dahl in running the experiments reported here is greatly appreciated. The authors would also like to acknowledge many helpful discussions with Dr. J. E. Broadwell. This work was sponsored by the Air Force Office of Scientific Research under Contract F49620-79-C-0159 and Grant 83-0213.

## References

- Mungal, M. G., Dimotakis, P. E., and Broadwell, J. E., "Turbulent Mixing and Combustion in a Reacting Shear Layer," *AIAA Journal*, Vol. 22, June 1984, pp. 797–800.
- Mungal, M. G. and Dimotakis, P. E., "Mixing and Combustion with Low Heat Release in a Turbulent Shear Layer," *Journal of Fluid Mechanics*, Vol. 148, 1984, pp. 349–382.
- Mungal, M. G., Hermanson, J. C., and Dimotakis, P. E., "Reynolds Number Effects on Mixing and Combustion in a Reacting Shear Layer," *AIAA Journal*, Vol. 23, Sept. 1985, pp. 1418–1423.
- Hermanson, J. C., "Heat Release Effects in a Turbulent, Reacting Shear Layer," Ph.D. Thesis, California Institute of Technology, Pasadena, CA, 1985.
- Koochesfahani, M. M. and Dimotakis, P. E., "Mixing and Chemical Reactions in a Turbulent Liquid Mixing Layer," *Journal of Fluid Mechanics*, Vol. 170, 1986, pp. 83–112.
- Brown, G. L. and Roshko, A., "On Density Effects and Large Structure in Turbulent Mixing Layers," *Journal of Fluid Mechanics*, Vol. 64, No. 4, 1974, pp. 775–816.
- Bernal, L. P., Breidenthal, R. E., Brown, G. L., Konrad, J. H., and Roshko, A., "On the Development of Three-Dimensional Small Scales in Turbulent Mixing Layers," *Turbulent Shear Flows 2, Second Symposium on Turbulent Shear Flows*, July 1979, Springer-Verlag, Berlin, pp. 305–313.
- Breidenthal, R. E., "Structure in Turbulent Mixing Layers and Wakes Using a Chemical Reaction," *Journal of Fluid Mechanics*, Vol. 109, 1981, pp. 1–24.
- Konrad, J. H., "An Experimental Investigation of Mixing in Two-Dimensional Turbulent Shear Flows with Application to Diffusion-Limited Chemical Reactions," Ph.D. Thesis, California Institute of Technology, Pasadena, CA, 1976; also, Project SQUID Tech. Rept. CIT-8-PU, 1976.
- Caldwell, F. R., "Thermocouple Materials," National Bureau of Standards Monograph 40, U.S. Department of Commerce, National Bureau of Standards, 1962.
- Scadron, M. D. and Warshawsky, I., "Experimental Determination of Time Constants and Nusselt Numbers for Bare-Wire Thermocouples in High-Velocity Air Streams and Analytic Approximation of Conduction and Radiation Errors," NACA Tech. Note 2599, 1952.
- Rebollo, M. R., "Analytical and Experimental Investigation of a Turbulent Mixing Layer of Different Gases in a Pressure Gradient," Ph.D. Thesis, California Institute of Technology, Pasadena, CA, 1973.
- Kee, R. J., Miller, J. A., and Jefferson, T. H., "CHEMKIN: A General Purpose, Problem Independent, Transportable, Fortran Chemical Kinetics Code Package," Sandia Labs., Livermore, CA, Rept. SAND80-8003, 1980.
- Cohen, N. and Bott, J. F., "Review of Rate Data for Reactions of Interest in HF and DF Lasers," The Aerospace Corporation, CA, Rept. SD-TR-82-86, 1982.
- Baulch, D. L., Duxbury, J., Grant, S. J., and Montague, D. C., "Evaluated Kinetic Data for High Temperature Reactions," *Journal of Physical Chemistry*, Vol. 4, 1981; Reference data in Vol. 10, Suppl. 1, 1981.
- Mungal, M. G. and Frieler, C. E., "The Effects of Damköhler Number on a Turbulent Shear Layer—Experimental Results," GALCIT, California Institute of Technology, Pasadena, CA, Rept. FM85-01, 1985.
- Wallace, A. K., "Experimental Investigation of the Effects of Chemical Heat Release in the Reacting Turbulent Plane Shear Layer," Ph.D. Thesis, University of Adelaide, 1981; also AFOSR Report AFOSR-TR-84-0650.
- Dimotakis, P. E., "Entrainment into a Fully Developed, Two-Dimensional Shear Layer," *AIAA Journal*, Vol. 24, Sept. 1986, pp. 1791–1796.
- McMurtry, P. A., Jou, W-H., Riley, J. J., and Metcalfe, R. W., "Direct Numerical Simulations of a Reacting Mixing Layer with Chemical Heat Release," *AIAA Journal*, Vol. 24, June 1986, pp. 962–970.
- Pitz, R. W. and Daily, J. W., "Combustion in a Turbulent Mixing Layer Formed at a Rearward-Facing Step," *AIAA Journal*, Vol. 21, Nov. 1983, pp. 1565–1570.
- Keller, J. O. and Daily, J. W., "The Effect of Large Heat Release on a Two Dimensional Mixing Layer," *AIAA Paper* 83-0472, 1983.
- Browand, F. K. and Latigo, B. O., "Growth of the Two-Dimensional Mixing Layer from a Turbulent and Non-Turbulent Boundary Layer," *The Physics of Fluids*, Vol. 22, No. 6, June 1979, pp. 1011–1019.
- Batt, R. G., "Some Measurements on the Effect of Tripping the Two-Dimensional Shear Layer," *AIAA Journal*, Vol. 13, Feb. 1975, pp. 245–247.
- Bradshaw, P., "The Effect of Initial Conditions on the Development of a Free Shear Layer," *Journal of Fluid Mechanics*, Vol. 26, No. 2, 1966, pp. 225–236.
- Ho, C. M. and Huerre, P., "Perturbed Free Shear Layers," *Annual Review of Fluid Mechanics*, Vol. 16, 1984, pp. 365–424.
- Brown, J. L., "Heterogeneous Turbulent Mixing Layer Investigations Utilizing a 2-D 2-Color Laser Doppler Anemometer and Using a Concentration Probe," Ph.D. Thesis, University of Missouri, Columbia, MO, 1978.
- Ganji, A. T. and Sawyer, R. F., "Experimental Study of the Flowfield of a Two-Dimensional Premixed Turbulent Flame," *AIAA Journal*, Vol. 18, July 1980, pp. 817–824.
- Libby, P. A. and Bray, K. N. C., "Countergradient Diffusion in Premixed Turbulent Flames," *AIAA Journal*, Vol. 19, Feb. 1981, pp. 205–213.
- Spalding, D. B., "The Two-Fluid Model of Turbulence Applied to Combustion Phenomena," *AIAA Journal*, Vol. 24, June 1986, pp. 876–884.